

Photovoltaic emulator using error adjustment fuzzy logic proportional-integral controller

Razman Ayop¹, Chee Wei Tan¹, Shahrin Md Ayob¹, Nik Din Muhamad¹, Jasrul Jamani Jamian¹, Zulkarnain Ahmad Noorden^{1,2}

¹School of Electrical Engineering, Universiti Teknologi Malaysia, Johor, Malaysia

²Institute of High Voltage and High Current, School of Electrical Engineering, Faculty of Engineering, Universiti Teknologi Malaysia, Johor, Malaysia

Article Info

Article history:

Received Oct 5, 2021

Revised Feb 10, 2022

Accepted Feb 25, 2022

Keywords:

Buck converter

Fuzzy logic controller

Photovoltaic

Proportional-integral controller

Single diode model

ABSTRACT

The photovoltaic (PV) technology has been increasingly used in our energy generation. Therefore, it is essential to have a good PV testing facility during the development process. The PV emulator (PVE) is a voltage or current source that mimic the current-voltage characteristic as a PV module that requires proper control strategy to work. The resistance feedback method (RFM) control strategy has many good attributes, except the transient response, which is caused by the proportional-integral (PI) controller. This paper proposed a new fuzzy logic PI (FLPI) controller to improve the transient performance of the RFM PVE. It is based on the error adjustment method that founded on the transient state and load of the PVE. The performance of the proposed PVE is compared with the original PVE that used RFM with the PI controller. The finding of the research shows that the transient performance of the proposed PVE has improved 2.3 times compared to the original PVE without affecting its accuracy.

This is an open access article under the [CC BY-SA](https://creativecommons.org/licenses/by-sa/4.0/) license.



Corresponding Author:

Razman Ayop

Division of Power, School of Electrical Engineering, Faculty of Engineering

Universiti Teknologi Malaysia

81310, UTM Johor Bahru, Johor, Malaysia

Email: razman.ayop@utm.my

1. INTRODUCTION

Nowadays, the use of photovoltaic (PV) technology is rapidly increasing [1]. This significant change is due to the government policy to reduce carbon dioxide emissions and ultimately reduce the effect of climate change. The development of the PV generation system such as solar charger and solar inverter is not an easy task. This is due to the low efficiency of the PV module, which results in a high-power requirement to test the system. The solar simulator used to test the PV module also has low efficiency. To overcome this inefficient testing problem, the PV emulator (PVE) is used.

The PVE is a voltage or current source that generate a close current-voltage (I-V) characteristic as the PV module. Five components need to be considered when it comes to the PVE. One of the components is the control strategy. The purpose of the control strategy is to obtain the reference point for the PVE. The control strategy determines the reference input of the closed-loop controller for the power converter in the PVE based on the load, irradiance, and module temperature. The common control strategy is the direct referencing method (DRM) [2]–[4]. The DRM is a simple control strategy and does not require any additional algorithm. Nevertheless, it has stability issues at the certain condition and the tuning of the closed-loop controller for the power converter is difficult since the control strategy is not robust (the control strategy affects the closed-loop controller for the power converter). Numerous control strategies have been suggested

to mitigate this problem. Among the control strategies, the resistance feedback method (RFM) has better advantages in various performances [5]–[7]. However, the transient performance of the RFM is lower compared to the DRM. This is due to the use of the proportional-integral (PI) controller as the closed-loop controller for the power converter in the RFM. The fuzzy logic (FL) controller has been implemented in many applications and has the potential to overcome this problem [8], [9].

There are several approaches to implementing the FL for the power converter. The first approach is to use the FL controller alone, as shown in Figure 1. The output of the FL controller determines the operation of the buck converter. The output produced is either the duty cycle [10], [11] or the change in the duty cycle [12], [13]. However, relying on the FL controller alone may result in inaccurate output [14]. The accuracy of the FL controller is improved by combining this controller with the PI or proportional-integral-derivative (PID) controller. By referring to Figure 1, the FL controller is used to adjust the gains of the PID controller [15]–[17] or adjusting the error before entered the PID controller [18]. Since the main concern for the PVE is the accuracy, the fuzzy logic proportional-integral (FLPI) or fuzzy logic proportional-integral-derivative (FLPID) controllers are recommended for the PVE.

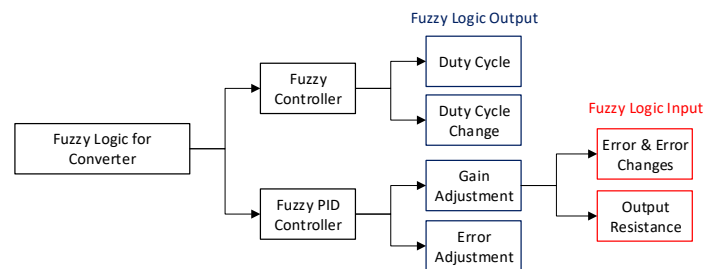


Figure 1. The approach in implementing FL controller for the converter

Currently, the PVE that uses the FLPI or FLPID controllers is based on the DRM as the control strategy. The tuning of the FLPI or FLPID controllers is difficult for PVE using DRM since the DRM is not a robust control strategy. The PVE using gain adjustment FLPID controller with the error and the change in error inputs requires three separate fuzzy controllers, where each fuzzy controller has 49 rules [17]. The high number of rules requires high processing power, this increases the computation time. The high computation time needs to be avoided since it can result in a fail emulation. The PVE using gain adjustment FLPI controller with the resistance input has a low number of rules [15]. Nevertheless, the tuned fuzzy controller may change at different irradiance. This method is improved using resistance and irradiance as input for the FLPI controller [19]. However, the complex relationship between the resistance, irradiance, and PI gains resulting the used of the artificial neural network to tune the FL controller. This requires large data and data training. The PVE using error adjustment FLPI controller with the error and the change in error inputs requires a high number of rules [18]. Still, this method has a good transient response.

The DRM has a fast response as the output resistance increases. This is due to the large reference input produce during the transient state, which produces a very large error and causing the PI controller to respond faster. Since RFM response slower as the output resistance increases, the fast characteristic of the DRM during high output resistance is needed in the RFM. The large error during the transient state and high output resistance is realized by implementing the FLPI controller based on error adjustment into the RFM. The rules for the FLPI controller are simpler since the RFM is not affected by the irradiance and the transient characteristic is predictable.

This paper proposed a new type of FLPI controller for the PVE using the RFM control strategy. The new FLPI is based on the error adjustment output and resistance-state input, which is based on the transient characteristic of the DRM. The proposed RFM PVE using the FLPI controller is compared with the original RFM PVE using the PI controller. The closed-loop current-controlled buck converter system is used for the PVE and it operates in the continuous current mode. The common single diode model with the 255 W power rating is used for the PVE. The proposed FLPI controller needs to have three inputs, which is the reference input, error, and output resistance. The reference and error inputs are used to detect the transient state. While the output resistance input is to detect the load condition. The aim is to produce a large error for the RFM during the transient period and high output resistance. The proposed method is expected to have a low number of rules for the FL controller and a good transient response for a wide load range. The next section reviews the methodology of the proposed RFM PVE using the FLPI controller. Section 3 shows the original

RFM PVE using the PI controller. Section 4 analyse the results and discuss the findings. The last section concludes the results based on the objectives.

2. PROPOSED PHOTOVOLTAIC EMULATOR

The proposed PVE uses the RFM integrated with the new FLPI controller that used transient state input to improve the transient performance. The PVE consists of various components such as the control strategy, current-resistance (I R) PV model, buck converter, PI controller, and FLPI controller. The contribution of the proposed PVE is on the new approach on designing the FPLI controller.

2.1. Control strategy

The proposed PVE is based on the RFM control strategy integrated with the FLPI controller. The FLPI controller is a new approach due to the state, S_t , input shown in Figure 2. The output voltage (V_o) and output current (I_o) is measured at the load. The output resistance (R_o) is digitally calculated and the result is used by the I-R PV model to calculate the reference current, I_{ref} . The I_{ref} is compared with the I_o to produce the error, e . The transient state, S_t , is calculated using (1). The S_t shows the current transient phase, in which zero is the initial phase and one is the final or steady phase. The FL controller obtains the R_o and S_t and produces the error gain, K_e . The K_e is multiplied with the e and the adjusted error, e_{adj} , is given to the input of the PI controller. The PI controller uses the e_{adj} and generate the duty cycle, D , and the corresponding switching pulse, sp is generated by the pulse width modulation (PWM). The sp switches the MOSFET in the buck converter, which changes the V_o and I_o . The process is repeated until I_{ref} is equal to I_o .

$$S_t = 1 - |e|/I_{ref} \tag{1}$$

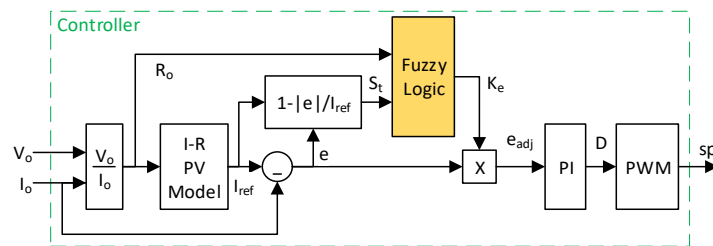


Figure 2. The proposed PVE using the RFM integrated with the FLPI controller

2.2. Current-resistance photovoltaic model

The RFM method involves a special kind of PV model named the I-R PV model [20]–[22]. This is different from the conventional PV model, which uses voltage or current as the input. The original I-R PV model is based on the look-up table since it cannot be solved by the standard Newton-Raphson method [22]. Then, this model is computed using the reverse triangular number [21], with a high computation requirement. The computation is improved using a root-finding method called the binary search method [20]. Therefore, the binary search method is chosen to compute the I-R PV model. The I-R PV model has PV resistance, R_{pv} , as the input and PV current, I_{pv} , as the output, as shown in (2). Several theoretical parameters such as saturated current (I_s), series resistance (R_s), parallel resistance (R_p), ideality factor (A), and thermal voltage (V_t) are obtained using the parameter extraction method.

$$I_{pv} = I_{ph} - I_s \left[\exp \left(\frac{I_{pv}(R_{pv}-R_s)}{AV_t} \right) - 1 \right] - \frac{I_{pv}(R_{pv}-R_s)}{R_p} \tag{2}$$

2.3. Buck converter

The buck converter shown in Figure 3 is intended to operate in the continuous current mode and the output voltage ripple factor, γ_{v_o} , is less than 1%. These two desired specifications are determined by the inductance (L) and capacitance (C). The L and C are calculated using (3) and (4), respectively [23]. The input voltage, V_i , needs to be higher than the output voltage during maximum output resistance ($R_{o,max}$), $V_{o,Ro,max}$. The switching frequency, f_s , is set to 30 kHz. While the minimum duty cycle, D_{min} , is set to 0.2, which higher D_{min} reduce the C and enhance the transient performance. The L and C are 210 μ H and 150 μ F, respectively.

$$L = \frac{\left(1 - \frac{V_{o,Ro,max}}{V_i}\right) R_{o,max}}{2f_s} \tag{3}$$

$$C = \frac{1-D_{min}}{8LYV_o f_s^2} \tag{4}$$

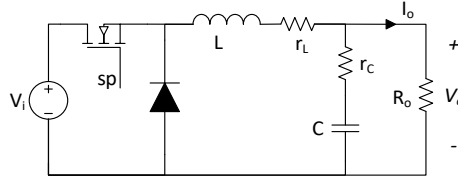


Figure 3. The schematic circuit of the buck converter

2.4. Proportional-integral controller

The transfer function of the PI controller, $G_c(s)$, is shown in (5), which consist of proportional gain (K_p) and integral gain (K_i). To properly adjust the K_p and K_i , the transfer function of the buck converter, $G_b(s)$, is needed, as provided in (6). The K_p and K_i are designed by utilizing the single input single output (SISO) tools provided in the simulation software.

$$G_c(s) = \frac{\hat{d}(s)}{\hat{e}_f(s)} = \frac{K_p s + K_i}{s} \tag{5}$$

$$G_b(s) = \frac{\hat{i}_o(s)}{\hat{d}(s)} = \frac{V_i}{R_o} \frac{(LC)^{-1}}{s^2 + (R_o C)^{-1} s + (LC)^{-1}} \tag{6}$$

2.5. Fuzzy logic controller

The proposed FLPI controller is a new approach based on the S_t input. This FLPI controller is based on the property of the DRM. However, the instability problem faced by the DRM is removed by manipulating the rules in the FL. Since the PVE requires both V_o and I_o sensors, the R_o input for the FL controller is not a problem.

The FL controller consists of dual inputs and single output. The input of the FL controller is the R_o and S_t . While the output of the FL controller is the K_e , which is multiply to e and goes into the PI controller to become the FPLI controller. The FP controller requires nine membership functions, which each input and output consists of three membership functions, as described in Figures 4 (a)–(c). Various types of membership function can be used and the performance is not significantly affected by the type of the membership function used. For this FL controller, the two Gaussian membership functions are chosen for all input and output. The S_t range is set from zero to one, in which zero is the initial state in the transient period and one is the final stage of the transient state. The R_o input is set within the range of load for the PVE, which is from 1 Ω to 18 Ω . The K_e output needs to start from one. The upper limit depends on the stability of the V_o and I_o . For this case, a maximum K_e of five is the maximum to create a stable output at the lower R_o .

After the membership functions are implemented into the FL controller, the rules need to be configured. The FL rules matrix is shown in Table 1. When the R_o is low, the K_e is unity, which means that the PI controller works normally. As the R_o increases, the K_e increase when the S_t is low. Nonetheless, as the S_t reaches a steady period, the K_e becomes unity to avoid instability problems.

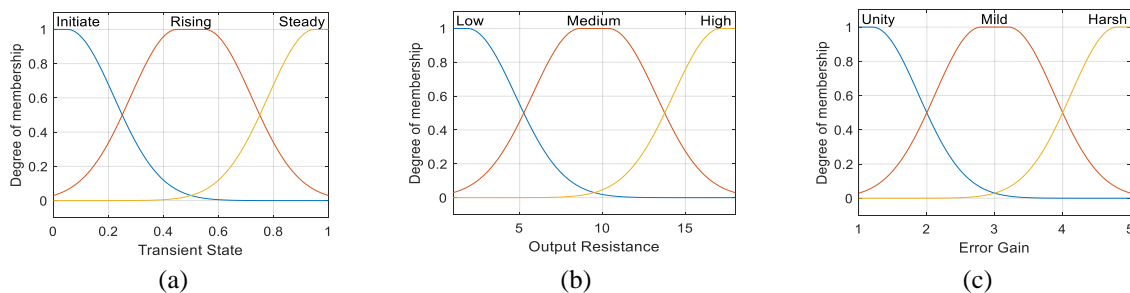


Figure 4. The membership functions of the FL controller (a) transient state, S_t (b) output resistance, R_o , and (c) error gain, K_e

Table 1. The FL rules matrix

Output Resistance/Transient State	Initiate	Rising	Steady
Low	Unity	Unity	Unity
Medium	Mild	Mild	Unity
High	Harsh	Mild	Unity

3. ORIGINAL PHOTOVOLTAIC EMULATOR

The original PVE is the RFM using the PI controller [5]. The design of the original PVE is similar to the proposed PVE except for the control strategy, in which the PVE lack of FL controller. The control strategy for the original PVE is shown in Figure 5. All the parameters used in the original PVE are similar to the proposed PVE to ensure a fair comparison.

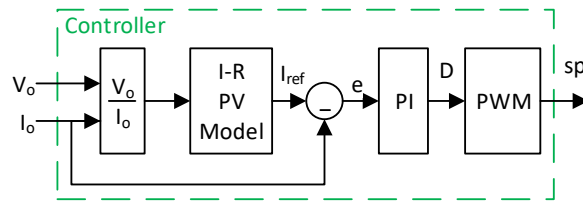


Figure 5. The proposed PVE using the RFM integrated with the PI controller

4. RESULTS AND DISCUSSION

The objective of the proposed PVE is to improve the transient performance of the original PVEs. Therefore, the transient response is analysed for both the proposed and the original PVE. Nevertheless, accuracy is a main factor for the PVE. Therefore, the accuracy for both proposed and original PVEs is tested to ensure both PI and FLPI controllers do not affect the accuracy of the PVE.

4.1. Accuracy

The accuracy is a significant feature for the PVE. A good closed-loop controller for the power converter should be able to produce V_o and I_o similar to a PV model [24]. By referring to Figure 6 (a), both proposed and original PVEs can mimic the I-V characteristic curve of the PV model. This demonstrates that the proposed and original PVE can operate correctly. Nonetheless, this result has low sensitivity when it comes to error analysis. Therefore, the percentage current error, $e_{i\%}$, is calculated using (7).

$$e_{i\%} = |I_o - I_{pv}| / I_{pv} \times 100\% \tag{7}$$

The $e_{i\%}$ is analysed at various R_o and the result is plotted in Figure 6 (b). The result shows that the maximum $e_{i\%}$ is 1% at low R_o . After 6 Ω , the $e_{i\%}$ is only around 0.15%. The reason $e_{i\%}$ is high when the R_o is low is because of the y_{Vo} . By referring to (4), lower D gives higher y_{Vo} when the C is kept constant. Since the D of a PVE is low when the R_o is low, this results in a higher y_{Vo} . This results in a higher $e_{i\%}$. The result also shows that proposed and original PVEs has similar $e_{i\%}$. This means that the proposed FLPI controller with S_i input does not affect the accuracy of the PVE.

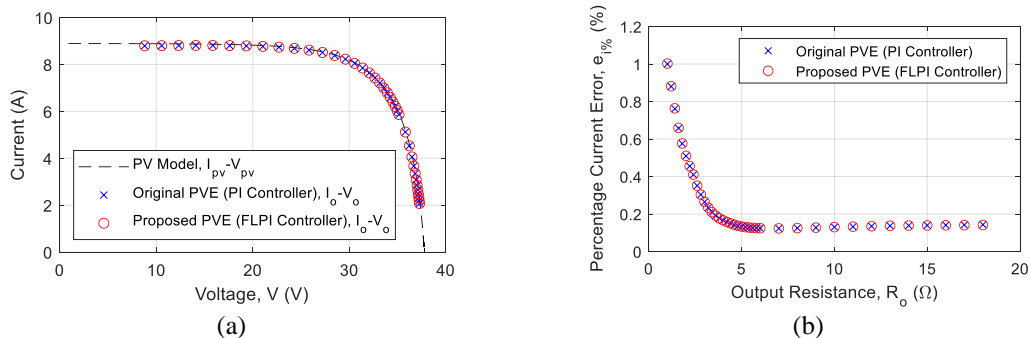


Figure 6. The accuracy of the PVE using the conventional PI and proposed FLPI controllers at 1000 W/m² and 25 °C (a) the I-V characteristic curve and (b) the corresponding $e_{i\%}$ against R_o

4.2. Transient response

The transient performance of the PVEs is measured using the settling time, t_s , which the settling time is the time taken for the I_o to reach 2% within its final value [25]. The t_s is observed for both proposed and original PVEs at the minimum and maximum R_o , 1 Ω and 18 Ω , respectively. The waveforms of the I_o are shown in Figure 7(a) and Figure 7(b).

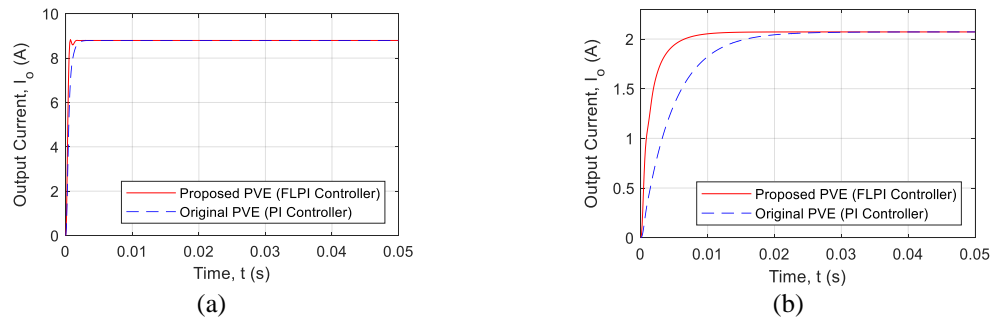


Figure 7. The waveform of I_o against time for the conventional PI and proposed FLPI controllers (a) 1 Ω output resistance and (b) 18 Ω output resistance

When the R_o is 1 Ω , the t_s for the proposed and original PVEs is 1.2 ms and 1.7 ms, respectively. At low R_o , the transient response is almost similar for proposed and original PVEs. This is because the proposed FL controller produces one K_e , which mean that the e_{adj} is equal to e , resulting in a similar result to the PI controller. However, when the R_o is 18 Ω , the t_s for the proposed and original PVEs is 7.9 ms and 18.3 ms, respectively. This shows that the proposed PVE is 2.3 times faster compared to the original PVE. This is due to the proposed FL controller that increases the K_e during the transient period, increasing the e_{adj} , and producing a faster response.

5. CONCLUSION

The objective of this study is to investigate the potential of the FL controller for the PVE that used the RFM control strategy. The original RFM uses the PI controller, which has a slower transient response as the load increased. The FLPI controller is introduced to overcome this problem. A new type of FLPI controller is introduced that requires a low number of membership functions and rules, which relates to a lower computation burden. This controller is based on the error adjustment technique, load, and transient state. The proposed FLPI controller for the PVE is proven to be effective since the transient response is 2.3 times faster compared to the PI controller when the load is high. The accuracy of the PVE is also not affected by the proposed FLPI controller. In conclusion, the proposed FLPI has a low computation burden and fast transient response without affecting the accuracy of the PVE.

ACKNOWLEDGEMENTS

The authors would like to express gratitude to Universiti Teknologi Malaysia (UTM) for providing comprehensive library facilities and funding. Funding provided by Universiti Teknologi Malaysia Encouragement Research Grant under vote Q.J130000.2651.18J39. Lastly, thanks to colleagues who have either directly or indirectly contributed to the completion of this work.




REFERENCES

- [1] REN21, "Renewables 2021 Global Status Report (GSR)," *Renewable Energy Policy Network for the 21st Century (REN21)*, 2021.
- [2] F. Barra *et al.*, "Dynamic and Reconfigurable Photovoltaic Emulator Based on FPAA," in *20th IMEKO TC4 International Symposium and 18th International Workshop on ADC Modelling and Testing Research on Electric and Electronic Measurement for the Economic*, Benevento, Italy, September 2014, pp. 1005–1010. [Online] Available: <https://www.imeko.org/publications/tc4-2014/IMEKO-TC4-2014-319.pdf>.
- [3] M. C. Di Piazza, M. Pucci, A. Ragusa, and G. Vitale, "Analytical Versus Neural Real-Time Simulation of a Photovoltaic Generator Based on a DC-DC Converter," in *IEEE Transactions on Industry Applications*, vol. 46, no. 6, pp. 2501–2510, November–December 2010, doi: 10.1109/TIA.2010.2072975.
- [4] A. Koran, K. Sano, R. Kim, and J. Lai, "Design of a Photovoltaic Simulator with a Novel Reference Signal Generator and Two-Stage LC Output Filter," in *IEEE Transactions on Power Electronics*, vol. 25, no. 5, pp. 1331–1338, May 2010, doi: 10.1109/TPEL.2009.2037501.




- [5] R. Ayop and C. W. Tan, "A novel photovoltaic emulator based on current-resistor model using binary search computation," *Solar Energy*, vol. 160, pp. 186–199, 2018, doi: 10.1016/j.solener.2017.12.005.
- [6] M. Farahani, M. A. Shamsi-nejad, and H. R. Najafi, "Design and construction of a digital solar array simulator with fast dynamics and high performance," *Solar Energy*, vol. 196, pp. 319–326, 2020, doi: 10.1016/j.solener.2019.12.032.
- [7] P. Garg, Priyanshi, and G. Bhuvanewari, "Power electronic circuit based implementation of a solar PV emulator using a power factor corrected buck converter," *2018 IEEMA Engineer Infinite Conference (eTechNxT)*, 2018, pp. 1–6, doi: 10.1109/ETECHNXT.2018.8385297.
- [8] D. Subhi and R. Thabit, "A New Low Cost Solar Array Emulator Based on Fuzzy and 32-Bit Microcontroller," *International Journal of Science and Engineering Investigations*, vol. 9, no. 101, pp. 63–69, June 2020, [Online] Available: <http://www.ijsei.com/papers/ijsei-910120-10.pdf>.
- [9] M. Alaoui, H. Maker, A. Mouhsen, and H. Hihi, "Photovoltaic emulator of different solar array configurations under partial shading conditions using damping injection controller" *International Journal of Power Electronics and Drive System (IJPEDS)* vol. 11, no. 2, pp. 1019–1030, June 2020, doi: 10.11591/ijpeds.v11.i2.pp1019-1030.
- [10] I. Atacak and O. F. Bay, "A type-2 fuzzy logic controller design for buck and boost DC–DC converters," *Journal of Intelligent Manufacturing*, vol. 23, no. 4, pp. 1023–1034, August 2012, doi: 10.1007/s10845-010-0388-1.
- [11] T. Gupta, R. R. Boudreaux, R. M. Nelms, and J. Y. Hung, "Implementation of a fuzzy controller for DC–DC converters using an inexpensive 8-b microcontroller," in *IEEE Transactions on Industrial Electronics*, vol. 44, no. 5, pp. 661–669, October 1997, doi: 10.1109/41.633467.
- [12] J. Lorenzo, J. C. Espiritu, J. Mediavillo, S. J. Dy, and R. B. Caldo, "Development and implementation of fuzzy logic using microcontroller for buck and boost DC–to–DC converter," in *IOP Conference Series: Earth and Environmental Science*, vol. 69, no. 1, 2017, p. 012193, doi: 10.1088/1755-1315/69/1/012193.
- [13] B. U. Patil and S. R. Jagtap, "Adaptive fuzzy logic controller for buck converter," *2015 International Conference on Computation of Power, Energy, Information and Communication (ICCPEIC)*, 2015, pp. 0078–0082, doi: 10.1109/ICCPEIC.2015.7259444.
- [14] S. Vinod, M. Balaji, and M. Prabhakar, "Robust control of parallel buck fed buck converter using hybrid fuzzy PI controller," *2015 IEEE 11th International Conference on Power Electronics and Drive Systems*, 2015, pp. 347–351, doi: 10.1109/PEDS.2015.7203509.
- [15] J. Zhang, S. Wang, Z. Wang, and L. Tian, "Design and realization of a digital PV simulator with a push-pull forward circuit," *Journal of Power Electronics*, vol. 14, no. 3, pp. 444–457, 2014, doi: 10.6113/JPE.2014.14.3.444.
- [16] C. S. Betancor-Martin, J. Sosa, J. A. Montiel-Nelson, and A. Vega-Martinez, "Gains tuning of a PI-Fuzzy controller by genetic algorithms," *Engineering Computations*, vol. 31, no. 6, pp. 1074–1097, 2014, doi: 10.1108/EC-03-2012-0068.
- [17] W. Shao, Z. Q. Meng, H. A. Zhou, and K. Zhang, "A photovoltaic array simulator based on current feedback fuzzy PID control," *Journal of Intelligent and Fuzzy Systems*, vol. 29, no. 6, pp. 2555–2564, 2015, doi: 10.3233/IFS-151958.
- [18] M. T. Iqbal, M. Tariq, and M. S. U. Khan, "Fuzzy logic control of buck converter for photo voltaic emulator," in *2016 4th International Conference on the Development in the in Renewable Energy Technology (ICDRET)*, 2016, pp. 1–6, doi: 10.1109/ICDRET.2016.7421477.
- [19] R. Ayop and C. W. Tan, "An Adaptive Controller for Photovoltaic Emulator using Artificial Neural Network," *Indonesian Journal of Electrical Engineering and Computer Science*, vol. 5, no. 3, pp. 556–563, March 2017, doi: <http://doi.org/10.11591/ijeecs.v5.i3.pp556-563>.
- [20] R. Ayop, C. W. Tan, and A. L. Bakar, "Simple and fast computation photovoltaic emulator using shift controller," *IET Renewable Power Generation*, vol. 14, no. 11, pp. 2017–2026, 2020, doi: 10.1049/iet-rpg.2019.1504.
- [21] R. Ayop, C. W. Tan, and K. Y. Lau, "Computation of current-resistance photovoltaic model using reverse triangular number for photovoltaic emulator application," *Indonesian Journal of Electrical Engineering and Informatics (IJEI)*, vol. 7, no. 2, pp. 314–322, June 2019, doi: 10.11591/ijeie.v7i2.1148.
- [22] P. H. To and D. Q. Phan, "A photovoltaic emulator using dSPACE controller with simple control method and fast response time," *2017 International Conference on System Science and Engineering (ICSSE)*, 2017, pp. 718–723, doi: 10.1109/ICSSE.2017.8030970.
- [23] R. Ayop, C. W. Tan, S. N. S. Nasir, K. Y. Lau and C. L. Toh, "Buck Converter Design for Photovoltaic Emulator Application," *2020 IEEE International Conference on Power and Energy (PECon)*, 2020, pp. 293–298, doi: 10.1109/PECon48942.2020.9314582.
- [24] I. Moussa and A. Khedher, "Photovoltaic emulator based on PV simulator RT implementation using XSG tools for an FPGA control: Theory and experimentation," *International Transactions on Electrical Energy Systems*, p. e12024, 2019, doi: 10.1002/2050-7038.12024.
- [25] I. D. G. Jayawardana, C. N. M. Ho, M. Pokharel, and G. Escobar, "A fast dynamic photovoltaic simulator with instantaneous output impedance matching controller," in *2017 IEEE Energy Conversion Congress and Exposition (ECCE)*, 1-5 Oct. 2017 2017, pp. 5126-5132, doi: 10.1109/ECCE.2017.8096863.

BIOGRAPHIES OF AUTHORS






Razman Ayop    received the bachelor's degree in electrical engineering with first-class honours, the master's degree in electrical engineering with specialization in power system, and the PhD degree in electrical engineering from Universiti Teknologi Malaysia (UTM), Johor, Malaysia, in 2013, 2015, and 2018, respectively. He is a Senior Lecturer with UTM and a member of Power Electronics and Drives Research Group, School of Electrical Engineering, Faculty of Engineering, UTM. His research interests include renewable energy and power electronics. He can be contacted at email: razman.ayop@utm.my.






Chee Wei Tan    received his B.Eng. degree in Electrical Engineering (First Class Honors) from Universiti Teknologi Malaysia (UTM), in 2003 and a Ph.D. degree in Electrical Engineering from Imperial College London, London, U.K., in 2008. He is currently an associate professor at Universiti Teknologi Malaysia and a member of the Power Electronics and Drives Research Group, School of Electrical Engineering, Faculty of Engineering. His research interests include the application of power electronics in renewable/alternative energy systems, control of power electronics and energy management system in microgrids. He can be contacted at email: cheewei@utm.my.






Shahrin Md Ayob    was born in Kuala Lumpur, Malaysia. He obtained his first degree in Electrical Engineering, Master in Electrical Engineering (Power), and Doctor of Philosophy (Ph.D.) from Universiti Teknologi Malaysia in 2001, 2003, and 2009, respectively. Currently, he is an associate professor at the School of Electrical Engineering, Faculty of Engineering, Universiti Teknologi Malaysia. He is a registered Graduate Engineer under the Board of Engineer Malaysia (BEM) and Senior Member of IEEE. His current research interest is the solar photovoltaic system, electric vehicle technology, fuzzy system, and evolutionary algorithms for power electronics applications. He can be contacted at email: e-shahrin@utm.my.






Nik Din Muhamad    is a lecturer at the Universiti Teknologi Malaysia, Johor, Malaysia since 1989 and the director of the Electrical Machine Laboratory there. His research focuses on Modeling, design and control of DC-DC converters. He earned a B. Eng from Universiti Teknologi Malaysia and and M. Eng in electrical engineering from the same university. He can be contacted at email: nikd@utm.my.



Jasrul Jamani Jamian    received the Bachelor of Engineering (B. Eng. (Hons)) degree, Master of Engineering (M. Eng.) and Ph.D degree in electrical (power) engineering from Universiti Teknologi Malaysia in 2008, 2010 and 2013 respectively. He is currently director for Power Engineering Division, School of Electrical Engineering, Universiti Teknologi Malaysia. Dr Jasrul is actively involved in research as a principal investigator as well as leader in consultancy projects with several companies such as Petronas and Tenaga Nasional Berhad, which focuses on relay coordination projects and off grid solar PV design. His research interest includes Network Reconfiguration, Optimization technique, and Renewable Energy. He can be contacted at email: jasrul@utm.my.



Zulkarnain Ahmad Noorden    received the B.Eng. and M.Eng. degrees in Electrical Engineering from Universiti Teknologi Malaysia (UTM) in 2008 and 2009, respectively. In 2013, he completed the Ph.D. degree in Regional Environment System (Electrical Engineering) from Shibaura Institute of Technology, Tokyo, Japan. Currently, he is a Senior Lecturer at the School of Electrical Engineering and Research Fellow at the Institute of High Voltage and High Current in UTM Johor Bahru, Malaysia. His research interests include ultracapacitor, energy storage systems, power equipment diagnosis, photovoltaic and high voltage. He can be contacted at email: zulkarnain-an@utm.my.